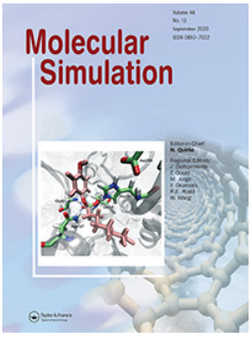

Molecular Simulation

ISSN: (Print) (Online) Journal homepage: https://www.tandfonline.com/loi/gmos20

A molecular dynamics simulation framework for predicting noise in solid-state nanopores

Onkar Patil , D. Manikandan & Vishal V. R. Nandigana

To cite this article: Onkar Patil , D. Manikandan & Vishal V. R. Nandigana (2020) A molecular dynamics simulation framework for predicting noise in solid-state nanopores, Molecular Simulation, 46:13, 1011-1016, DOI: 10.1080/08927022.2020.1798004

To link to this article: https://doi.org/10.1080/08927022.2020.1798004

MOLECULAR SIMULATION
2020, VOL. 46, NO. 13, 1011–1016
https://doi.org/10.1080/08927022.2020.1798004

A molecular dynamics simulation framework for predicting noise in solid-state nanopores

Onkar Patil, D. Manikandan and Vishal V. R. Nandigana

Fluid Systems Laboratory, Department of Mechanical Engineering, Indian Institute of Technology, Madras, Chennai, India

ABSTRACT

In this paper, we perform all-atom molecular dynamics (AA-MD) simulations to predict noise in solid-state nanopores. The simulation system consists of ~70,000 to ~350,000 atoms. The simulations are carried out for ~1.3 μs over ~6500 CPU hours in 128 processors (Intel® E5-2670 2.6 GHz Processor). We observe low and high frequency noise in solid-state nanopores. The low frequency noise is due to the surface charge density of the nanopore. The high frequency noise is due to the thermal motion of ions and dielectric material of the solid-state nanopore. We propose a generalised noise theory to match both the low and high frequency noise. The study may help ways to study noise in solid-state nanoporous membranes using MD simulations.

ARTICLE HISTORY
Received 1 March 2020
Accepted 13 July 2020

KEYWORDS
Noise; molecular dynamics; nanopores

1. Introduction

Nanofluidics is the study and manipulation of fluids confined within 1–100 nm [1–4]. The behaviour of fluid changes at the nanoscale compared to the bulk scale, because atomic and molecular interactions between solid-liquid interfaces play a significant role at such small length scales. Over the last decade, nanofluidics has made giant strides in applications like DNA sequencing [5–8], seawater desalination [9–12], liquid electronics [13–15], and nanofluidic diodes [16–20]. The solid-state nanopores, however exhibit significantly higher noise than the biological membranes and hence act as a roadblock for many of these applications [21–23]. The origin of the noise was postulated as surface charge fluctuations [24,25], nanochannel's opening and closing processes in the case of track etched membranes [26], the formation of nanobubble inside the nanopore [27], and cooperative effect on ion motion inside confined geometry [28]. In this paper, we propose all-atom molecular dynamics simulations (AA-MD) framework [29–32] to predict noise inside solid-state nanopores. Any statistical fluctuation of current or voltage may be quantified by the variance, its square root, the standard deviation, or the power spectral density (PSD) which also considers the frequency (f) dependence. The variance is calculated as the integral of the PSD over a bandwidth (B). We measure the PSD from ionic current-time data for solid-state nanopores and discuss the origin of the noise.

2. Simulation details

First, the silicon nitrinde (Si_3N_4) slab of dimension 6.19 nm × 6.19 nm × 4.64 nm (and 15.4 nm × 15.4 nm × 4.64 nm) is created by replicating cubic unit cell of γ-Si_3N_4 [33] in three dimensions. To drill a nanopore of diameters 3.56, 5.2, and 10.16 nm, the centre of the pore is chosen in such a way resulting in a uniform circular nanopore. The creation of the pore led to the non-zero charge of the Si_3N_4 slab. In order to maintain electroneutrality of the Si_3N_4 slab, the partial charge of the Si atom was adjusted by 0.1%. In this work, we assume a uniform surface charge (σ) of −0.02, −0.2, and 2 C/m^2. To obtain the desired surface charge density (σ), additional charges were added to the surface atoms of the pore along with its partial charge (see Figure 1(a)). The entire Si_3N_4 slab is solvated, and K^+ and Cl^- ions were added using the autoionize VMD plugin [34]. Also, extra positive ions (K^+) were added inside the pore to make the system electroneutral. SPC/E water model was used to model the water molecules, and ions were modelled as the L-J particles. The non-bonded parameters for all-atom types are taken from ref [33]. Further, a cut off radius of 1.1 nm was used for non-bonded interactions. Also, the particle mesh Ewald (PME) with a grid space of 1.1 nm was used for computing electrostatic interactions. Furthermore, the AA-MD simulations are performed using NAMD 2.12 package [35]. The multi-time step (MTS) algorithm with a 1-2-4 fs time step was used for integrating Newton's equation of motion to get the trajectory of the atoms. The trajectories were recorded every 0.1 ps. Initially, the entire system undergoes the minimisation of 10,000 steps to reach a minimum energy configuration state. Then the system was equilibrated in NPT ensemble at atmospheric pressure and constant temperature for 3 ns. The final system after NPT simulation, having a total length of 17.98 nm is shown in Figure 1(b). We carried out all our simulation at 300 K using Langevin thermostat with a dampening coefficient of 0.1 ps^{-1}. The non-equilibrium simulation was performed by applying an external voltage under NVT

CONTACT Vishal V. R. Nandigana nandiga@iitm.ac.in Fluid Systems Laboratory, Department of Mechanical Engineering, Indian Institute of Technology, Madras, Chennai 600036, India

Supplemental data for this article can be accessed online at https://doi.org/10.1080/08927022.2020.1798004.
This article has been republished with minor changes. These changes do not impact the academic content of the article.

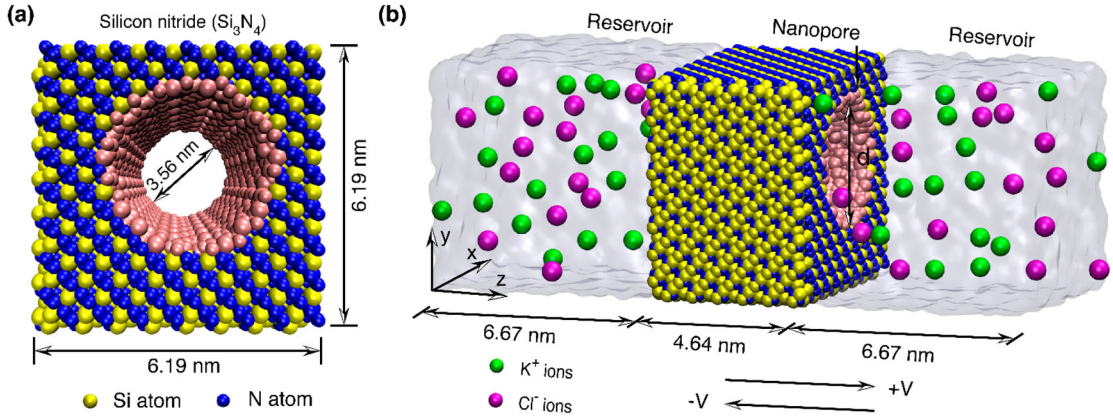

Figure 1. (Colour online) All-atom molecular dynamics (AA-MD) simulation setup. (a) A silicon nitride nanopore and (b) A final simulation setup indicates the size of the system after NPT simulation. Semitransparent surface indicates the water molecules.

ensemble. Each simulation was run for 100 ns. The large simulation time was used to gather good statistics to study low and high frequency noise.

3. Results and Discussions

3.1. I-V characteristics

A total of ~70,000 to ~350,000 atoms are simulated for a total time of ~1.3 µs in ~6500 hours CPU hours using 128 cores (Intel® E5-2670 2.6 GHz) processor. The ionic current is calculated inside the nanopore using Equation (1) [30–32]

$$I\left(t+\frac{T}{2}\right)=\frac{1}{TL}\sum_{i=1}^{N_P} q_i(z_i(t+T)-z_i(t)) \tag{1}$$

where $i = 1, 2, \ldots, N_P$, N_P is the total number of ions inside the nanopore, z_i and q_i are the z-coordinate and charge of ion, respectively. L is the length of the nanopore, and T is the sampling time. Figure 2(a) shows the variation of the current with time. Figure 2(b) shows the I–V characteristics of the solid-state nanopore for three different diameters (d). Here, the current follows the Ohm's law during both forward (+V) and reverse (−V) bias. For all the pore diameters considered, the aspect ratio (L/d) is less than 1.5. Due to such a low aspect ratio, we used a thin nanofluidic membrane equation to calculate the ionic conductance (G) and ionic current (I) [36–39]

$$G=K_b\left[\frac{4L}{\pi d^2}\frac{1}{1+4(l_{\mathrm{Du}}/d)}+\frac{2}{\gamma d+\beta l_{\mathrm{Du}}}\right]^{-1} \tag{2}$$

where K_b is the bulk conductivity, L is the pore length, d is the pore diameter, l_{Du} is the Dukhin length (which can be approximated by ($|\sigma/F|/2c_s$), where F is the Faraday's constant and c_s is the bulk concentration), γ is a geometrical prefactor that depends on the model used and β is a fitting parameter (here, $\gamma = 1$ and $\beta = -3$) to obtain the best match with the MD simulation results.

4. Low frequency noise – model

Figure 2 shows the power spectral density (PSD) of the ionic current calculated using Welch method [40]. The simulations show both low and high frequency noise. Note, in the experiments the frequency range typically studied is 1 Hz to 1 MHz. Further, the low frequency noise range is between 1 Hz and 1 kHz and the noise above 1 kHz is studied as high

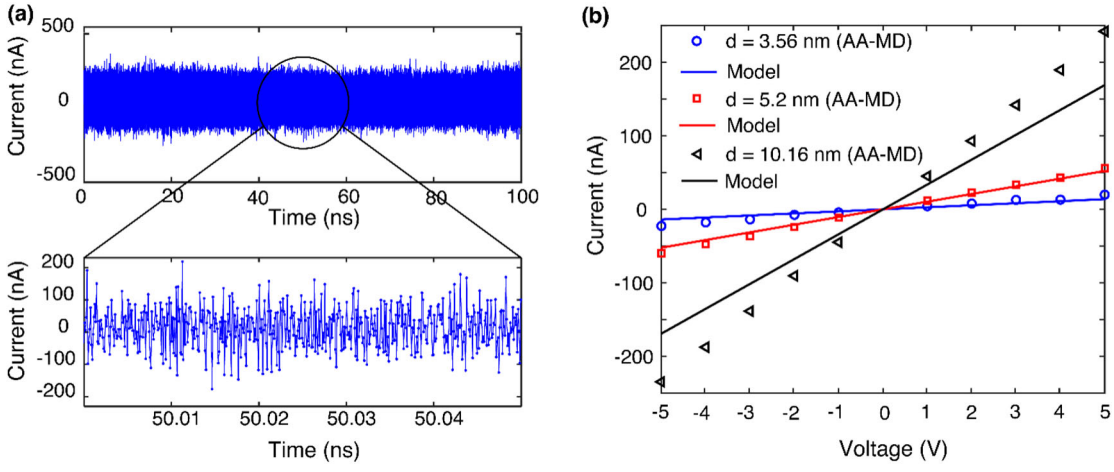

Figure 2. (Colour online) (a) Current oscillations of nanopore (d = 3.56 nm) for the applied voltage of 3 V corresponding to the surface charge of −0.2 C/m^2. (b) Shows the I–V characteristics for three different nanopore diameters.

frequency noise [41–50]. However in our simulations, owing to the computational limitations of MD, we took the length of the reservoir to be ~7 nm which is many orders smaller than a real experimental reservoir, hence the time scales are shifted compared to the real experimental system. For example, the longest relaxation time of the system is the diffusion time, which in our case is $(2L_{\text{reservoir}} + L)^2/6D$ where, $L_{\text{reservoir}}$ is the length of the reservoir, L as discussed before is the pore length. The longest relaxation time of the system is found to be ~ 26.9 ns. We ran our simulations for 100 ns so that we can capture the longest relaxation time. The low frequency noise regime is the reciprocal of the longest relaxation time which is ~ 37.12 MHz. Also, the high frequency limit corresponds to the smallest relaxation time of the system. The drift of the ions dictates the smallest relaxation time of the system. In our simulations, the drift velocity of the ion is found to be ~ 289.6 m/s. The smallest relaxation time of the system is given by L/v, where v is the drift velocity of the ion inside the nanoporous membrane. The smallest relaxation time is found to be ~ 16 ps. We used a time step of 0.1 ps to record the current trajectory and thus, we are able to capture the smallest relaxation time and the high frequency regime of the system. Thus, one cannot directly consider the same time scales of the experiment with our simulations. However, the conclusions drawn from our simulations are same as the experimental results as the dimensions of the nanoporous membrane are in the same range as the experimental results [42].

For applied surface charge density (σ) of −0.2 C/m^2, Figure 3(c) shows that the low frequency noise scales as $1/f^{\alpha}$ with $\alpha \approx 0.65$. The results agree well with the literature where α is typically 0.5 to 1.5. To understand the origin of low frequency noise, we varied the surface charge density of the nanopore. When the surface charge density (σ) is 0 C/m^2, i.e. the charge on each atom of Si_3N_4 is zero, the factor α is found to be equal to 0.25 (see Figure 3(a)). The result revealed that surface charge density of the nanopore plays a major role in the scaling of the low frequency noise in solid-state nanopores. To confirm the result, we varied the surface charge density of the nanopore from $\sigma = -0.02$ C/m^2 to $\sigma = -2$ C/m^2. We observed that the factor α is almost constant, α varied between 0.65 and 0.7. The constant value of α is because the counter-ions are screened completely at such high surface charge densities, resulting in dominant surface conduction mode. To reconfirm if surface charge density of the nanopore and the surface conduction is the dominant mechanism for the origin of the low frequency noise, we varied the concentration between 0.5 and 5 M at $\sigma = -0.2$ C/m^2. For low concentrations from 0.5 M to 1 M, the factor α is found to be 0.65 and for high concentrations between 2 and 5 M, α is found to decrease to 0.35–0.25, respectively (see Figure 4(a)). The decrease in α at high concentration is due to the fact that the surface conduction mode becomes less dominant and the bulk conduction starts to dominate.

To model the low frequency noise, we use Hooge's phenomenological relation [51]. According to Hooge relation, noise power (A) scales inversely with the total number of charge carriers.

$$\frac{S_{IL}}{I^2} = \frac{A}{f} = \frac{\alpha'}{N_c f} \tag{3}$$

where S_{IL} is the PSD of the low frequency noise, I is the ionic current, α' is the Hooge parameter, N_c is the number of charge carriers which is directly proportional to bulk concentration, and A is the noise power. Figure S1(a) shows that the noise power (A) decreases with an increase in the salt concentration consistent with Equation (3). The slope of A with $1/N_c$ gives the Hooge parameter ($\alpha' = 8.41 \times 10^{-3}$) and is observed to be constant (see Figure S1(b)). For high bulk concentration (2 and 5 M), the noise power deviates from the linear variation due to the dominance of the bulk conduction.

5. High frequency noise – model

For the high frequency noise, we propose thermal noise and dielectric noise to be dominant source of noises. The two sources of noise are given by

$$S_{IH} = S_{IT} + S_{ID} \tag{4}$$

$$S_{IT} = \frac{4K_b T}{R_P} \tag{5}$$

$$S_{ID} = 8\pi K_b C_P T D f \tag{6}$$

where S_{IT} is the thermal noise (also called Johnson noise or shot noise or white noise) which arises from thermal motions of ions and is independent of frequency, S_{ID} term is a dielectric noise; the noise associated with the dielectric material of the nanopore, K_b is the Boltzmann constant, T is the temperature in K, D is the dielectric dissipation factor, R_P and C_P are the resistance and capacitance of the nanopore, respectively. To find the resistance (R_P) and the capacitance (C_P) of the nanopore, we approximate the entire simulation system as a hypothetical system. In such a system, the reservoir resistance (R_R) is assumed to be connected in series with parallel resistor-capacitor (R_P–C_P) circuit of the solid-state nanopore [42,50]. To determine the capacitance of the nanopore, we assume the nanopore as an ideal capacitor (i.e, dielectric dissipation factor (D) = 0, and $R_P = 0$) resulting a series reservoir resistance (R_R) – nanopore capacitor (C_P) circuit. The value of reservoir resistance (R_R) is obtained by simulating the reservoir alone filled with KCl solution. The reservoir resistance (R_R) is then subtracted from total resistance of the system ($R_{\text{Total}} = R_P + R_R$) to obtain the pore resistance (R_P). For a series R_R–C_P circuit, the initial decay rate of the ionic current, I_t is given by Equation (7) and is used to find the capacitance (C_P)

$$I_t = I_{\max} e^{(-t/R_R C_P)} \tag{7}$$

where $I_{\max}$ is the maximum current at the time, $t = 0$. We fit Equation (7) to ionic current obtained from AA-MD simulation and the capacitance of the nanopore was found to be 2.7868×10^{-18} F which is in close agreement with the theoretical value ($C_P = \varepsilon_o\, \varepsilon_r\, A/L$, where ε_o is the relative permittivity of the free space, ε_r is the dielectric constant of the nanopore material, A is the nanopore cross sectional area, and L is the length of the nanopore). The dielectric dissipation factor (D) is a free parameter which is the property of the nanopore material and is obtained by fitting the PSD with Equation (4). The dielecric dissipation factor (D) is found to be 0.003, which matches well with experimental dielectric dissipation

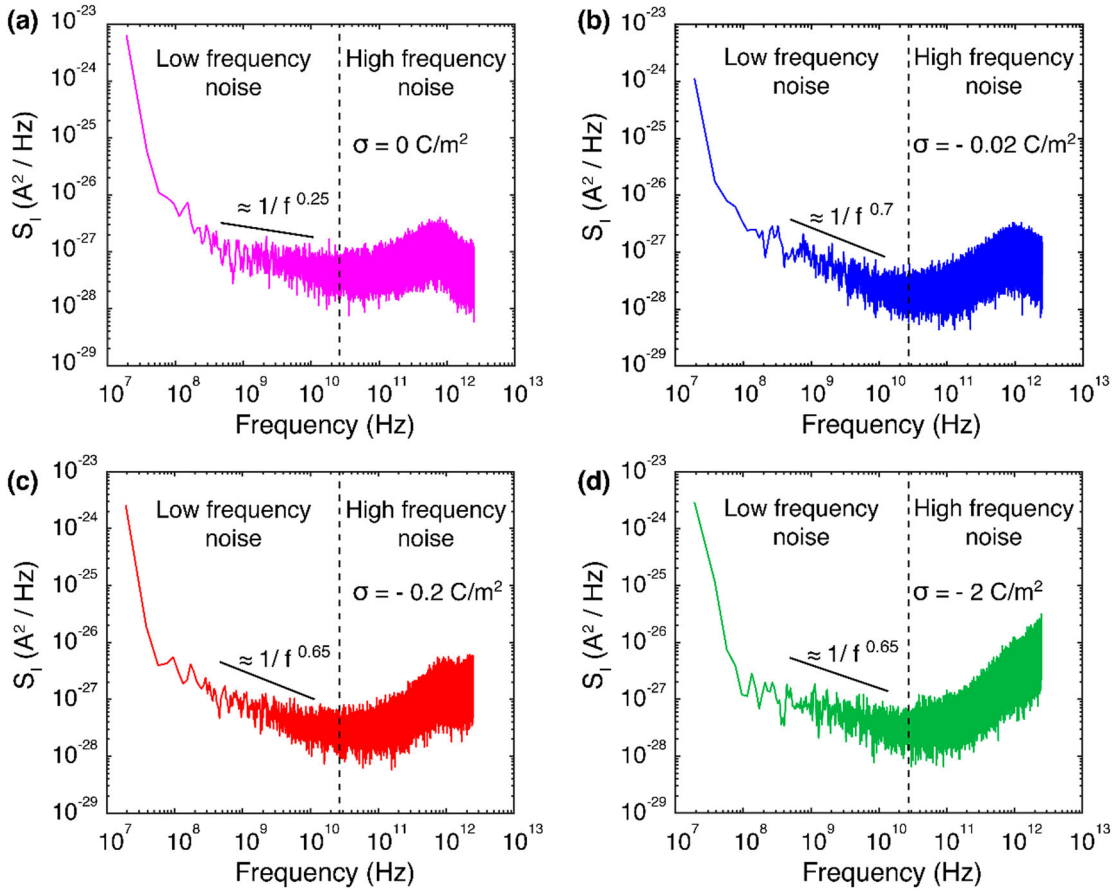

Figure 3. (Colour online) Power spectral density (PSD) for nanopore of diameter (d) = 3.56 nm corresponding to four different surface charge density under the applied voltage of 3 V. (a) $\sigma = 0$ C/m^2, (b) $\sigma = -0.02$ C/m^2, (c) $\sigma = -0.2$ C/m^2, and (d) $\sigma = -2$ C/m^2.

factor (D) for silicon nitride material [52,53]. Our theory for high frequency noise is further validated by fitting the theory with the simulation results (see Figure 4(b)).

Finally, a generalised noise theory to capture both low and high frequency noise in solid-state nanopores is given as

$$S_I = S_{IL} + S_{IH} = \frac{\alpha' I^2}{N_C f^{\alpha}} + \frac{4K_b T}{R_P} + 8\pi K_b C_P T D f \qquad (8)$$

The noise theory is validated by fitting the theory with the simulation results. Figure 4(b) shows the comparison between the simulation and theory and we see a good agreement between the two results. Further, to confirm the theory works well we fit the theory for different values of surface charge density of the nanopore (see Figure S3). We observe that the theory matches well with the simulations for capturing both low and high frequency noise. Furthermore, resistance-capacitance (R_R–C_P) noise, generally modelled in experiments [42] is absent

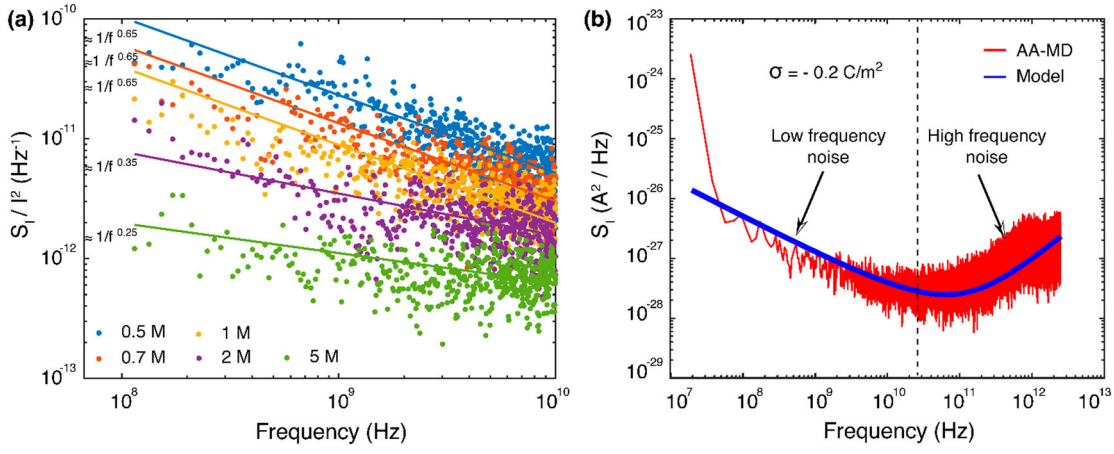

Figure 4. (Colour online) (a) Normalised power spectral density of nanopore (d = 3.56 nm) for five different concentrations, and (b) Shows the generalised noise theory predicting low and high frequency noise corresponding to the surface charge density of $\sigma = -0.2$ C/m^2 and the applied voltage of 3 V.

in our simulations, since we controlled the temperature of the reservoir and also the nanopore by using a Langevin thermostat [35] that reduced this source of noise.

6. Conclusion

In this paper we present a molecular dynamics simulation framework to predict the noise in solid-state nanopores. We found surface charge density as the main source of noise in low frequency noise regime and thermal and dielectric noises are the main sources of noise in high frequency regime. The study may help ways to study noise in solid-state nanoporous membranes using MD simulations.

Acknowledgements

This work was supported by IITM NFIG grant #MEE/17-18/862/NFIG/NADI, IITM NFSC grant #MEE/17-18/689/NFSC/NADI and Indo-US joint center grant #USSTF/JC-042/2017. The authors would like to acknowledge VIRGO and GNR computational resources provided by Indian Institute of Technology, Madras (IITM).

Disclosure statement

No potential conflict of interest was reported by the author(s).

Funding

This work was supported by IITM New Faculty Initiative Grant [grant number MEE/17-18/862/NFIG/NADI], IITM New Faculty Seed Grant [grant number MEE/17-18/689/NFSC/NADI] and Indo-US Science and Technology Forum [grant number USSTF/JC-042/2017].

ORCID

D. Manikandan http://orcid.org/0000-0002-3742-0047

References

[1] Eijkel JCT, Berg Avd. Nanofluidics: what is it and what can we expect from it? Microfluid Nanofluidics. 2005;1:249–267.
[2] Bocquet L, Charlaix E. Nanofluidics, from bulk to interfaces. Chem Soc Rev. 2010;39:1073–1095.
[3] Schoch RB, Han J, Renaud P. Transport phenomena in nanofluidics. Rev Mod Phys. 2008;80:839–883.
[4] Dekker C. Solid-state nanopores. Nat Nanotechnol. 2007;2:209–216.
[5] Heerema SJ, Vicarelli L, Pud S, et al. Probing DNA translocations with inplane current signals in a graphene nanoribbon with a nanopore. ACS Nano. 2018;12:2623–2633.
[6] Comer J, Aksimentiev A. DNA sequence-dependent ionic currents in ultra-small solid-state nanopores. Nanoscale. 2016;18:9600–9613.
[7] Comer J, Ho A, Aksimentiev A. Toward detection of DNA-bound proteins using solid-state nanopores: insights from computer simulations. Electrophoresis. 2012;33:3466–3479.
[8] Farimani AB, Dibaeinia P, Aluru NR. DNA origami–graphene hybrid nanopore for DNA detection. ACS Appl Mater Interfaces. 2017;9:92–100.
[9] Cohen-Tanugi D, Grossman JC. Water desalination across nanoporous graphene. Nano Lett. 2012;12:3602–3608.
[10] Heiranian M, Farimani AB, Aluru NR. Water desalination with a single-layer MoS_2 nanopore. Nat Commun. 2015;6:8616.
[11] Surwade SP, Smirnov SN, Vlassiouk IV, et al. Water desalination using nanoporous single-layer graphene. Nature Nanotech. 2015;10:459–464.
[12] Boretti A, Al-Zubaidy S, Vaclavikova M, et al. Outlook for graphene-based desalination membranes. NPJ Clean Water. 2018;1:5.
[13] Karnik R, Fan R, Yue M, et al. Electrostatic control of ions and molecules in nanofluidic transistors. Nano Lett. 2005;5:943–948.
[14] Radisavljevic B, Radenovic A, Brivio J, et al. Single-layer MoS_2 transistors. Nature Nanotech. 2011;6:147–150.
[15] Lopez-Sanchez O, Lembke D, Kayci M, et al. Ultrasensitive photodetectors based on monolayer MoS_2. Nature Nanotech. 2013;8:497–450.
[16] Siwy Z, Gu Y, Spohr HA, et al. Rectification and voltage gating of ion currents in a nanofabricated pore. Europhys Lett. 2002;60:349–355.
[17] Karnik R, Duan C, Castelino K, et al. Rectification of ionic current in a nanofluidic diode. Nano Lett. 2007;7:547–551.
[18] Vlassiouk I, Siwy ZS. Nanofluidic diode. Nano Lett. 2007;7:552–556.
[19] Yan R, Liang W, Fan R, et al. Nanofluidic diodes based on nanotube heterojunctions. Nano Lett. 2009;9:3820–3825.
[20] Nandigana VVR, Jo K, Timperman A, et al. Asymmetric-fluidic-reservoirs induced high rectification nanofluidic diode. Sci Rep. 2018;8:13941.
[21] Tabard-Cossa V, Trivedi D, Wiggin M, et al. Noise analysis and reduction in solid-state nanopores. Nanotechnology. 2007;18:305505.
[22] Soskine M, Biesemans A, Moeyaert B, et al. An engineered ClyA nanopore detects folded target proteins by selective external association and pore entry. Nano Lett. 2012;12:4895–4900.
[23] Mohammad MM, Iyer R, Howard KR, et al. Engineering a rigid protein tunnel for biomolecular detection. J Am Chem Soc. 2012;134:9521–9531.
[24] Smeets RMM, Dekker NH, Dekker C. Low-frequency noise in solid-state nanopores. Nanotechnology. 2009;20:095501.
[25] Hoogerheide DP, Garaj S, Golovchenko JA. Probing surface charge fluctuations with solid-state nanopores. Phys Rev Lett. 2009;102:5–8.
[26] Tasserit C, Koutsioubas A, Lairez D, et al. Pink noise of ionic conductance through single artificial nanopores revisited. Phys Rev Lett. 2010;105:260602.
[27] Smeets RMM, Keyser UF, Wu MY, et al. Nanobubbles in solid-state nanopores. Phys Rev Lett. 2006;97:088101.
[28] Siwy Z, Fuliński A. Origin of 1/fα noise in membrane channel currents. Phys Rev Lett. 2002;89:158101.
[29] Qiao R, Aluru NR. Ion concentrations and velocity profiles in nanochannel electroosmotic flows. J Chem Phys. 2013;118:4692–4701.
[30] Comer J, Dimitrov V, Zhao Q, et al. Microscopic mechanics of hairpin DNA translocation through synthetic nanopores. Biophys J. 2009;96:593–608.
[31] Cruz-Chú E, Aksimentiev A, Schulten K. Ionic current rectification through silica nanopores. Phys Chem C Nanomater Interfaces. 2009;113:1850.
[32] Aksimentiev A, Schulten K. Imaging α-hemolysin with molecular dynamics: ionic conductance, osmotic permeability, and the electrostatic potential map. Biophys J. 2005;88:3745–3761.
[33] Ho C, Qiao R, Heng JB, et al. Electrolytic transport through a synthetic nanometer-diameter pore. PNAS. 2005;102:10445–10450.
[34] Humphrey W, Dalke A, Schulten K. VMD: Visual molecular dynamics. J Mol Graph. 1996;14:33–38.
[35] Phillips JC, Braun R, Wang W, et al. Scalable molecular dynamics with NAMD. J Comput Chem. 2005;26:1781–1802.
[36] Lee C, Joly L, Siria A, et al. Large apparent electric size of solid-state nanopores due to spatially extended surface conduction. Nano Lett. 2012;12:4037–4044.
[37] Siria A, Poncharal P, Biance A-L, et al. Giant osmotic energy conversion measured in a single transmembrane boron nitride nanotube. Nature. 2013;494:455–458.
[38] Feng J, Graf M, Liu K, et al. Single-layer MoS_2 nanopores as nanopower generators. Nature. 2016;536:197–200.
[39] Macha M, Marion S, Nandigana VVR, et al. 2D materials as an emerging platform for nanopore-based power generation. Nat Rev Mater. 2019;1:1–18.
[40] Welch D. The use of fast fourier transform for the estimation of power spectra: a method based on time averaging over short, modified periodograms. IEEE Trans Audio ElectroacousticsAU. 1967;15:70–73.
[41] Levis RA, Rae JL. The use of quartz patch pipettes for low noise single channel recording. Biophys J. 1993;65:1666–1677.

[42] Smeets RMM, Keyser UF, Dekker NH, et al. Noise in solid-state nanopores. PNAS. 2008;105:417–421.
[43] Kumar A, Park K-B, Kim H-M, et al. Noise and its reduction in graphene based nanopore devices. Nanotechnology. 2013;24:495503.
[44] Balan A, Machielse B, Niedzwiecki D, et al. Improving signal-to-noise performance for DNA translocation in solid-state nanopores at MHz bandwidths. Nano Lett. 2014;14:7215–7220.
[45] Heerema SJ, Schneider GF, Rozemuller M, et al. 1/*f* noise in graphene nanopores. Nanotechnology. 2015;26:074001.
[46] Wen C, Zeng S, Arstila K, et al. Generalized noise study of solid-state nanopores at low frequencies. ACS Sensors. 2017;2:300–307.
[47] Fragasso A, Pud S, Dekker C. 1/*f* noise in solid-state nanopores is governed by access and surface regions. Nanotechnology. 2019;30:395202.
[48] Knowles SF, Keyser UF, Thorneywork AL. Noise properties of rectifying and non-rectifying nanopores. Nanotechnology. 2020;31:10LT01.
[49] Gravelle S, Netz RR, Bocquet L. Adsorption kinetics in open nanopores as a source of low-frequency noise. Nano Lett. 2019;19:7265–7272.
[50] Lianga S, Xianga F, Tang Z, et al. Noise in nanopore sensors: sources, models, reduction, and benchmarking. Nanotech and Precis Eng. 2020;3:9–17.
[51] Hooge FN. 1/*f* noise is no surface effect. Phys Lett. 1969;29A:139.
[52] Barta J, Manela M, Fischer R. Si_3N_4 and Si_2N_2O for high performance radomes. Mater Sci Eng. 1985;71:265–272.
[53] Lukianova OA, Sirota VV. Dielectric properties of silicon nitride ceramics produced by free sintering. Ceram Int. 2017;43:8284–8288.